

OBSERVATION OF THE 1970 MEXICO SOLAR ECLIPSE

Takumi Mori* and Yoshio Kubo*

Received 2 August 1971

Abstract

In the total solar eclipse of March 7, 1970, observation of contact times was made at Puerto Escondido in southern Mexico. The present paper gives the descriptions on the observations and the process of determining the apparent relative position of the sun to the moon.

The observation was made by the spectrophotometric method; the spectrograph was composed of an objective prism of a direct vision type, a telescope ($f=930$ mm, $\phi=58$ mm), and a 16 mm-movie camera. Registrations were made at a rate of 16 shots per second for 45 seconds around each contact, and good images of the flash spectra between 4500 Å and 5200 Å were obtained with precise time recordings.

Photographic measurements were carried out at 4615 Å on 60 frames for the 2nd contact and 100 for the 3rd. Photographic densities of the spectra were read out referring to the prominent features of the moon's limb to avoid the effects of image distortions. A curve of the limb darkening of the sun was obtained, which had the maximum gradient of 7.0 m per 1".

In order to compare the results of the observation with the limb profiles of Watts' charts, some small modifications were made to both the position angles and the heights in the charts, retaining their datum unmoved. The apparent relative position of the sun to the moon was determined finally on the basis of Watts' charts with the accuracies of $\pm 0.01''$ in the direction of the apparent relative motion and $\pm 0.1''$ in its perpendicular.

Between the observation results and the ephemeris some differences are found, which are difficult to be explained by the expected corrections to the adopted values of the ephemeris time and the geodetic position of the observation point.

1. Introduction

In principle, the relative position of the sun to the moon can be determined directly by observing the progress of a solar eclipse. The centers of both the sun and the moon are detected with reference to their respective limbs in this method. In truth, the sun has not a discontinuous boundary on the margin but gradually diminishes its intensity toward the outer region. In a certain region, however, the change in the intensity is so abrupt as to amount to 100 times per 1.0" along the radius. It seems to be somewhere in this region that is usually recognized as the solar edge (Although the definition of the solar edge is thus obscure within a

* Astronomical Division, Hydrographic Department.

very narrow limit, it does not mean any inconvenience for defining the center of the sun as long as the layers investigated are concentric and stable).

In the older days, the relative position of the sun to the moon was determined geometrically by measuring the photographic images of the sun in the partial phase on the plates taken by a long focal telescope. The greatest difficulties in the method were deformations of the images by turbulence of the earth's atmosphere and uncertain irregularities in the moon's profile.

The introduction of cinematographic technique in the 1920's was an epoch-making development in the history of eclipse observation; it replaced the geometrical method by an entirely new method which consists of measuring the amount of light employing the fact that it changes rapidly at the inner contacts and suffers comparatively little influence of the atmospheric turbulence. Furthermore, a number of reliable charts of the moon's profile were published recently.

The center of the moon, as far as it is derived from optical observation on the edge, can not be determined independently of a contour map. In other words, the center must be defined consistently with the datum of the contour map. The relation between the geometrical and dynamical centers of the moon should be determined as the results of the accumulation of such observations and the theoretical developments.

As stated above the contact problem is preferable to be treated photometrically and in actual observations the contact times are determined by measuring the intensity of light from the stable layers in the boundary regions of the solar surface. Since the observed quantity in this method is the integrated amount of light from all the layers outside the point considered, the light from, for example, the chromosphere, of which the layers are comparatively thick and unstable, has rather bad effects and should be rejected. It is therefore recommended that the stronger lines of the spectrum are avoided and the continuum only is used. In order to satisfy these conditions we have two methods: (1) spectral, and (2) using a monochromatic filter. When photography is used as the means of registration of the light, it is necessary to make the images have some area because the microphotometer demands a two dimensional expanse of the images for measurement. In the first method this condition is filled intrinsically, but in the second case it is necessary, for example, to let the images run by using a running camera.

In the 1970 Mexico Eclipse, the authors adopted the spectrophotometric method. The method has two advantages, as well as those mentioned, that it gives some data on the solar physics at the same time and that it does not require any expensive equipment especially designed. In the spectrophotometric method, the spectra of the crescents of the sun dispersed to the direction perpendicular to them are obtained by cinematographically at the inner contacts and the time of exposure for each photograph is recorded by time marks printed on the edge of the film. The intensity of the integrated light over any point on the moon's contour changes with time monotonously and, if a contact is defined by a certain amount of the

intensity, it can be determined for each contour point by following the successive frames.

Finally, if we know the times of the contacts for all the observed points on the moon's contour, the position of the sun is obtained relative to the datum of the moon's limb by the least squares determination.

The moon's contours taken from the charts do not in general coincide perfectly with the corresponding contours obtained from the observation. The differences may be caused by the image distortions and by the defects of the charts. The effect of the atmospheric disturbance is not so serious as other causes such as Eberhard effects. It is advisable that the contour map is revised slightly in order to take these effects into account, while the revised contour is kept coincident with the original one as a whole.

2. Equipments

It is desirable to record phenomena faithfully in detail just as they occur. On the other hand it is important also, especially in the field works, that the equipments are easy to handle and capable to get the data even under rather bad conditions. The system of the observational equipments was originally designed just to register the contacts with the accuracy such that the standard deviations for the final values of the moon's profiles were comparable to the uncertainties in the available charts of moon's profiles.

The observational system consists of a spectrotelescope, a 16 mm-movie camera, a timing device and an equatorial mounting (See Fig. 1.).

The spectrotelescope is of an objective direct vision type, which is composed of a SF2-60° prism and two BK7-38° unequal-sided ones on its both sides and an achromatic lens of 58 mm in aperture, 930 mm in focal length. This optical system is specified to make the light of 4860 Å pass without deflection and to yield a dispersion of about 100 Å per mm at H_{β} in the focal plane. The movie camera is one of Bolex H 16's, which was driven with an electric motor on the day. In order to set the plane of dispersion in the direction of the position angle of each inner contact, these two parts of the system are constructed to a rigid unit with iron tube, which is held at the center by the bearings on the equatorial mounting as to be rotated around the optical axis. Then measurement on the microphotometer becomes easier since direction of dispersion in the picture is always parallel to the frame works of the film.

The time signals of 50, 1, 0.1 and 1/60 Hz are generated by a crystal oscillator and are mixed and made into 0.3 m sec-width pulses through simple electronic circuits, which stimulate a miniature neon lamp in a small cylindrical capsule fixed in the camera. The flashes of the time signals thus yielded are printed as a sequence of small circular spots on a side line of the film through a pinhole of the capsule. The clock rate of the crystal oscillator is compared with the standard time signals

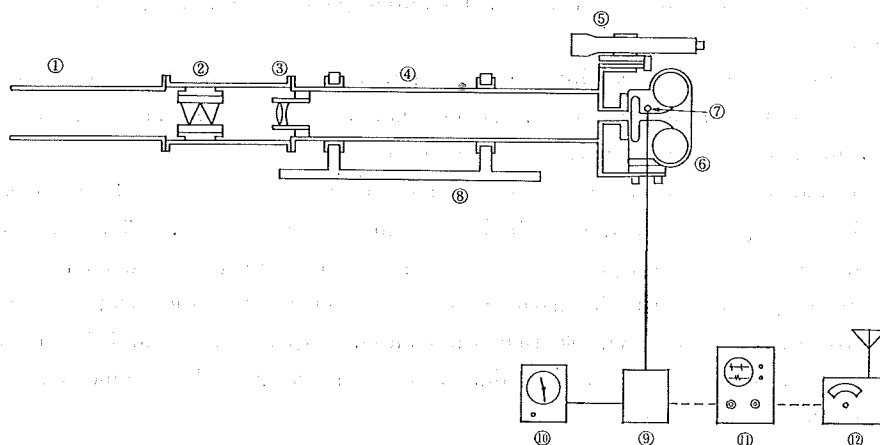


Fig. 1 The schematic diagram of the spectrophotographic equipments.

1. hood, 2. prisms, 3. lens, 4. telescope tube, 5. guiding telescope,
6. 16-mm movie camera, 7. miniature neon lamp, 8. bearings,
9. electronic circuits, 10. crystal clock, 11. dual beam synchroscope,
12. all wave receiver.

by means of photography on a dual beam synchroscope. The equatorial mounting is one of those of the same type being in use in the usual domestic field works, for example, of satellite geodesy. Its driving mechanism for diurnal motion is controlled by a tuning fork oscillator powered by dry cells.

3. Observation

All the Japanese expeditions, that is, those of Tokyo Astronomical Observatory, Kwasan Observatory and Hydrographic Department settled their observation stations at Puerto Escondido, a small village on the Pacific coast of southern Mexico. The camping site was in the yard of an electric power plant situated on a small plateau of about 100 m height where one can look down the Pacific Ocean some 1 km away in south and west.

The astronomical longitude and latitude of the station were determined through equal altitude observations by a Ni-2 type astrolabe of Carl Zeiss. The height was reduced by means of the trigonometric measurements from the mean sea level of Puerto Escondido Bay where the tidal heights were observed for 12 hours on a calm day.

In the morning of the 7th of March, the day of the solar eclipse, the meteorological condition was so favorable as could be. The meteorological observations on the station at 10^h40^m Mexico Standard Time, that is, 30 minutes before the second contact, furnished; cloud: 0, atmospheric pressure: 1007 mb, temperature: 31.3°C, humidity: 51.3%, wind: west, 3 in scale, transparency: best.

The self-registering thermometer recorded a maximum temperature of 31.8°C at 10^h27^m, which was followed by an abrupt linear decrease to the minimum of 27.5°C at

11^h42^m, 10 minutes after the third contact, and then occurred a quick recovery to the ordinary temperature of the month.

The observation of the eclipse was carried out successfully as had been scheduled beforehand; the flash spectra were photographed from 11^h26^m50^s to 11^h27^m35^s for the second contact and from 11^h30^m15^s to 11^h31^m02^s for the third with 16 shots per second. The time of exposure was 0.022^s. The exposures for calibration of the photographic density were made at 13^h10^m after the eclipse and finally a small experiment was made at 14^h00^m in the dark room of the camp.



Fig 2 Flash spectra

Fig. 2 shows a part of the film of the eclipse; the diameter of the moon is 9 mm in the original picture. The strongest line in the center of the spectrum is that of H_{β} and the magnesium triplet at some 5170 Å is seen in the right. In the sequence of the photographs we can see clearly that the intensity of the continuum shows so rapid decrease, while those of the emission lines change little with time. A sequence of the small circular spots on the side line of the film are the time signals of 50 Hz, where the break of the sequence means a right second.

After the end of the partial phase some exposures were made in order to convert photographic density into intensity of light. In the place of the telescopic hood in Fig. 1 (①) was set a 50 cm focal length collimator, which had a neutral glass wedge with density gradient of 0.15 per mm. Then the collimator was guided directly to the sun and shots were made with different slit widths under the same controls as in the photographings of the flash spectra.

In order to examine the positional relation between each photographic frame and its corresponding spot of time signal, the following small experiment was made after the field observation. Another miniature neon lamp connected seriesly with the lamp just used for printing the time marks in the camera was set on the objective side of the aperture of the camera. The camera was driven continuously while these two neon lamps were lighted on and off incessantly by one switch. In this case the simple photographic measurements on the developed film give the distance on the film between the spot and the photograph exposed at the same instant.

The film prepared for this observation was Eastman Plus-X Negative (16 mm, ASA 80 in day light).

The development of the film was made commercially at a domestic laboratory.

4. Photometry

The photometry was performed on the 60 successive photographs about the second contact and 100 about the third. These numbers of the photographs correspond to

4^s and 6^s of registration time interval, respectively. The color region swept by the slit of the microphotometer was near 4615 Å, which was located rather near to the edge of the picture but was not affected by any stronger emission line. The best focus was attained unexpectedly at this wavelength.

The measurements were carried out by means of a Nalumi self recording microphotometer of Tokyo Astronomical Observatory by the courtesy of the staffs of the observatory. The scanning was made rectilinearly in the right angle to the dispersion. The recording speed was 140 mm per minute on the role paper on which the enlargement of the picture was 160 to 1 and the density range covered was between 0.27 and 2.27.

The dimension of the slit used was 16" × 80"; the former figure corresponds to 0.2° of the position angle at the limb of the moon and the latter to 6 Å in the spectrum.

These measurements were performed in one day and night, in which period a picture of a step wedge was swept several times to check the performance of the system, and there was no discernible indications of the drift. Since the rectilinear sweep caused small shift of the wavelength measured, the corrections for this effect were evaluated by measuring a few pictures of the flash spectra at the two regions of 4615 Å and 4633 Å. The result shows no significant differences of the photographic densities between these two color regions.

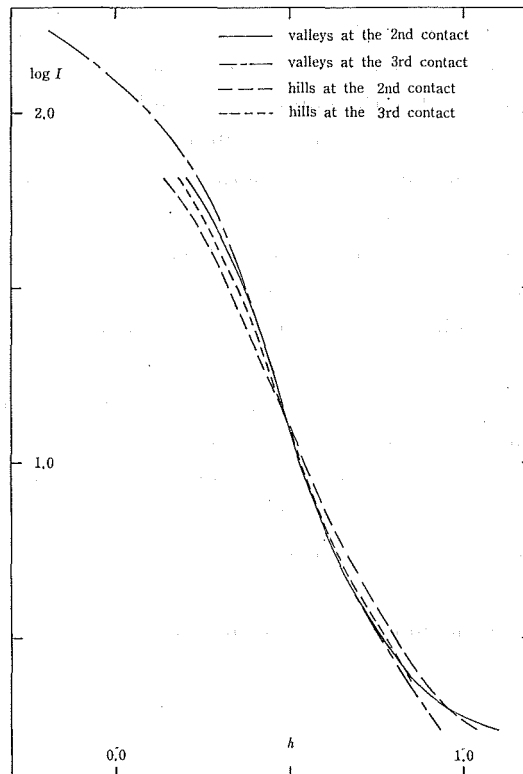


Fig. 3 Intensity gradients at the extreme disk of the sun.

In Fig. 3 are given the gradients of the limb-darkening obtained at 4615 Å. For the purpose of fixing the eyes always on the same radii of the sun, the densities of the points in the pictures corresponding to the same distinct hills and valleys of the moon were read out from the recording paper, and the continuous series of readings thus gained were reduced to $\log I$, I being intensity of light in an arbitrary scale, with respect to the photospheric height. There we can see some discrepancies especially at the top and the bottom of the curves among those of the hills and valleys for the second and the third contacts. They are, of course, not real. We should remember that those portions of the curves were derived from the registrations out of the proper exposures and furthermore that the observation was made with a rather small optical system. Therefore we cannot have any absolute confidence upon these figure, but we can estimate coarsely the magnitude of the darkening in the extremity of the photosphere. $d \log I / dh$ takes the maximum value of 2.8 at the inflection points of the curves, where h means the photospheric height. Or we may write in the form

$dm/dh=7.0$ m/second of arc,	at 4615 Å,
which is compared with	
$dm/dh=5.69 \pm .11$	at 4100 Å (Kristenson),
4.86	at 4800 Å (Lindblad),
10.5	at 6190 Å (Kristenson).

Since the definition of the solar edge is essentially arbitrary in a sense of photometry, we shall not intend to discuss on the radius of the sun in the present paper, but define the contact, for convenience, by a certain value of the density. If we could define the edge by the inflection point of the curve in Fig. 3, the final value of the radius of the sun shown later (Sec. 5-13) should be reduced by 0.04".

5. Data Processing

1) Apparent relative positions

In order to compare the observed relative positions with the ephemeris, the exact values must be known for the ephemeris time and the geodetic position of the observation point. However a large amount of accumulation of the astronomical and the geodetic observations is necessary before those values come to be available. So, the studies on this thema being left for the subsequent reports, the apparent relative position of the sun to the moon only is discussed in the present paper. For the convenience of the future studies, however, the results of the present investigation shall be expressed in such a form that they can be compared with the ephemeris as soon as the necessary values become to be known.

In the present paper, ΔT and the geodetic coordinates of the observation point are assumed to have the following values:

$\Delta T \equiv ET - UTC$	+38.8 ^s ,
the geodetic coordinates	
longitude	97° 04' 24.75" W,

latitude $15^{\circ} 51' 53.60''$ N,
 height above the sea level 93.1^m ,

The latter are the values obtained astronomically and trigonometrically as stated in Section 3.

The adopted constants (IAU, 1964) are:

the flattening of the earth $1/298.25$,
 the radius of the moon 0.2725026
 in the unit of the equatorial radius of the earth.

From these values adopted the topocentric ephemeris of the sun and the moon are:

at $17^h 27^m 15.566^s$ UTC (which is t_{02} as defined later);

$\alpha_{\odot} = 23^h 11^m 10.158^s$, $\alpha_{\zeta} = 23^h 11^m 08.933^s$,
 $\delta_{\odot} = -5^{\circ} 14' 27.19''$, $\delta_{\zeta} = -5^{\circ} 15' 02.70''$,
 $r_{\odot} = 16' 06.84''$, $r_{\zeta} = 16' 47.66''$.

These are calculated from the Japanese Ephemeris for 1970 which includes corrections to the new IAU system. (0's are supposed formally, if necessary, after the lowest decimals of the figures.)

2) Fundamental Equations

After Kristenson (1951) we derive the fundamental equations for determining the apparent relative position of the sun with respect to the moon. Consider a time t_{02}

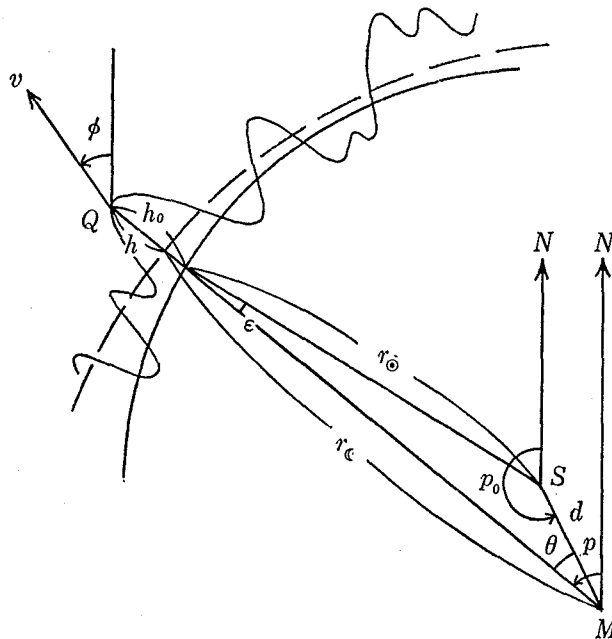


Fig. 4 Relation between the sun and the moon.

S, M : the centers of the sun and the moon respectively,
 r_{\odot}, r_{ζ} : the radii of the sun and the moon respectively,
 N : the direction of the north pole.

near the second contact. Fig. 4 shows the relative positions of the sun and the moon at t_{02} . In the figure h_0 is the height of a point Q on the lunar contour of which the position angle is p above the solar edge.

Let t_c be the time at which this contour point Q touches the solar edge. Denoting the speed and the direction of the motion of the moon to the sun by v and ϕ respectively, we get

$$h_0 = -v \cos(\phi - p) \times (t_c - t_{02}). \quad (1)$$

Also with d denote the distance between the centers of the sun and the moon and with h the height of the point Q above the zero level of the lunar limb, then

$$r_\odot \cos \varepsilon + h_0 + d \cos(p_0 - p - 180^\circ) = r_\zeta + h.$$

The meaning of ε is shown in the figure and p_0 is the position angle of the center of the moon with respect to that of the sun. Developing $\cos \varepsilon$ we can write

$$d \cos(p_0 - p) + (r_\zeta - r_\odot) = h_0 - r_\odot \frac{\varepsilon^2}{2} - h.$$

When any contour map is available, we can read from it the height h_M for the corresponding position angle. Writing

$$h = h_M + h',$$

we have

$$d \cos(p_0 - p) + (r_\zeta - r_\odot) = h_0 - r_\odot \frac{\varepsilon^2}{2} - h_M - h'.$$

The residual height h' represents the error in the contour map.

In the equation, put

$$\begin{aligned} d \cos p_0 &= x_2, & \cos p &= a, \\ d \sin p_0 &= y_2, & \sin p &= b, \\ r_\zeta - r_\odot &= z_2, & r_\odot \frac{\varepsilon^2}{2} &= \nu, \end{aligned}$$

then, using (1)

$$ax_2 + by_2 + z_2 = -v \cos(\phi - p) \times (t_c - t_{02}) - \nu - h_M - h',$$

where we can write

$$\nu = r_\odot \frac{\varepsilon^2}{2} = \frac{d^2}{2r_\odot} \sin^2 \theta.$$

Similarly for the third contact, we have

$$ax_3 + by_3 + z_3 = -v \cos(\phi - p) \times (t_c - t_{03}) - \nu - h_M - h'.$$

In the equations, however, x_2 , y_2 , z_2 , x_3 , y_3 and z_3 are not all independent of each other, but are connected by the following relations,

$$\begin{aligned} x_3 - x_2 &\equiv \xi = (\delta_\zeta - \delta_\odot)_{03} - (\delta_\zeta - \delta_\odot)_{02}, \\ y_3 - y_2 &\equiv \eta = \{(\alpha_\zeta - \alpha_\odot)_{03} - (\alpha_\zeta - \alpha_\odot)_{02}\} \cos \delta_\odot, \\ z_3 - z_2 &\equiv \zeta = (r_\zeta - r_\odot)_{03} - (r_\zeta - r_\odot)_{02}. \end{aligned}$$

The suffixes 02 and 03 mean the values at t_{02} and t_{03} , respectively.

The quantities $(\delta_\zeta - \delta_\odot)_{02}$, $(\delta_\zeta - \delta_\odot)_{03}$ and similar ones in the right-hand sides, themselves are unknown—they are the very quantities to be determined—, but their differences or ξ , η and ζ are known from the predictions.

Thus we obtain the fundamental equations

$$\begin{aligned}
 ax_2 + by_2 + z_2 &= -v \cos(\phi - p) \times (t_c - t_{02}) - \nu - h_M - h' & (2) \\
 &\text{(for the second contact)} \\
 ax_2 + by_2 + z_2 &= -v \cos(\phi - p) \times (t_c - t_{03}) - \nu - h_M - h' - a\xi - b\eta - \zeta \\
 &\text{(for the third contact),}
 \end{aligned}$$

where v and ϕ are slightly different between at the second and the third contacts, and the respective values must be used.

It is suggestive to express the relative positions in terms of the two components, one along the direction of the relative motion and the other perpendicular to it. In this case the first component is expected to be determined with a much better accuracy. By simple mathematical relations

$$\begin{aligned}
 x &= x' \cos \phi + y' \sin \phi, \\
 y &= x' \sin \phi - y' \cos \phi,
 \end{aligned}$$

we transform (x, y) into (x', y') . Then obviously from Fig. 5, (x', y') are the components required. For ϕ the value at the second contact is used.

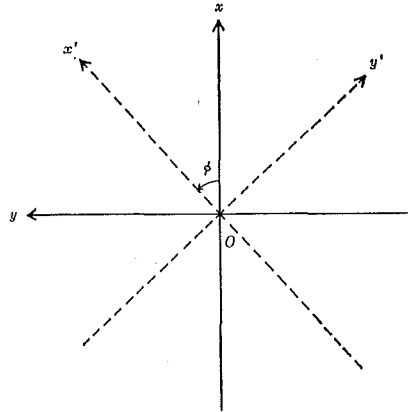


Fig. 5 Relation between (x, y) and (x', y') .

The equations become

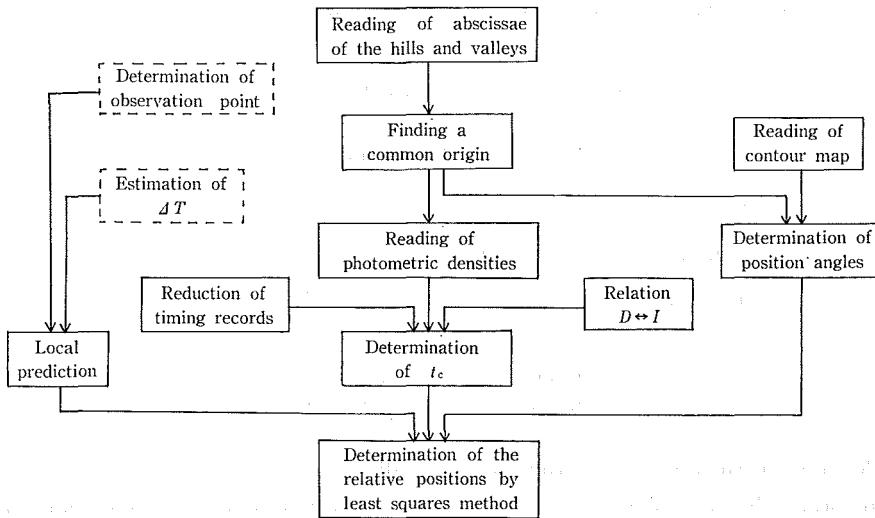
$$\begin{aligned}
 a'x_2' + b'y_2' + z_2 &= -v \cos(\phi - p) \times (t_c - t_{02}) - \nu - h_M - h' & (3) \\
 &\text{(for the second contact),} \\
 a'x_2' + b'y_2' + z_2 &= -v \cos(\phi - p) \times (t_c - t_{03}) - \nu - h_M - h' - a\xi - b\eta - \zeta \\
 &\text{(for the third contact),}
 \end{aligned}$$

where

$$a' = \cos(\phi - p), \quad b' = \sin(\phi - p).$$

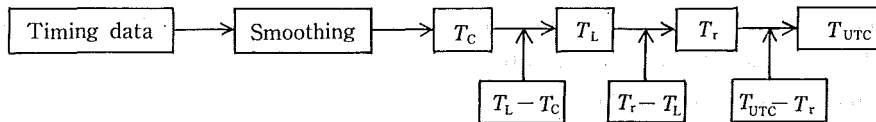
3) Flowchart for the data processing

The following schema shows the process of the reduction. A series of calculations must be carried out about the items shown in the schema. Most of the calculations have been made by HIPAC-103 of Hydrographic Department. The details of each calculation, except for those already mentioned, shall be discussed in order.



4) Reduction of the timing records

The moment of exposure for each frame of the flash spectrum is obtained by reading the spot mark of the neon lamp printed just beside the frame concerned. The raw timing data thus measured are smoothed and then reduced to the UTC system in the way which is shown in the following schema. The accuracy of the timing for each frame is better than 2 msec.



$T_L - T_c$: the time interval corresponding to the distance on the film from a frame to the mark which was recorded at the same instant as the exposure of the frame. The conversion factor from the distance to the time interval was determined with the accuracy higher than 1 msec by reducing the results of the test carried out in the dark room just after the observation of the eclipse.

$T_r - T_L$: the difference between the received WWV time signals and the pulses from the crystal clock.

$T_{UTC} - T_r$: the travel time between the WWV station in Fort Collins and Puerto Escondido.

5) Local predictions

In order to solve the least squares equations for determining the relative positions, it is necessary, as stated in 2), to know in advance the relative velocity and some other quantities. For this purpose the computing program for local predictions of solar

eclipse, which had been developed by the authors for planning the expedition, was applied with some minor modifications.

The necessary values thus obtained are shown in Table 1.

TABLE 1. PREDICTIONS

contact	t (UTC)	v	ϕ	d	p_0
second	17 ^h 27 ^m 15.566 ^s	0.3870"/sec	44.77°	39.95"	207.24°
third	17 ^h 30 ^m 31.536 ^s	0.3865"/sec	44.62°	39.51"	62.31°

$$\xi = +0.27490"/\text{sec} \times (t_{03} - t_{02}) = +53.872''$$

$$\eta = +0.27190"/\text{sec} \times (t_{03} - t_{02}) = +53.284''$$

$$\zeta = +0.00031"/\text{sec} \times (t_{03} - t_{02}) = +0.061''$$

6) Reading for the abscissae of the hills and valleys

In order that the photographic densities are measured for the same point on the moon's contour throughout all the frames, it is necessary that the position angle of any point on the contour are known for every frame. This is done by identifying some prominent hills and valleys for every frame and then comparing the means of their abscissae with a contour map.

In the actual case 18 hills and valleys, called "control points" hereafter, were chosen for each contact and they were compared with Watts' charts.

In any profile, all the control points do not appear at the same time. The control points could be measured only when their photographic densities were within the limit between 0.8 and 1.8. Moreover, sometimes the noises make it impossible to measure them even within the limit. The number of the control points in one frame of which the abscissae could be read was 5 to 10.

7) Finding a common origin

Since the abscissae of the profiles are read referring to the scale on the recording paper, the origin for each profile is not in general at the same position with respect to the control points. Therefore the process of taking an average among them is not necessarily trivial. In order to find out a common origin, all the profiles must be made coincide with each other by pursuing the control points appearing in the successive frames. Then the averages of the adjusted abscissae referred to this origin are taken for all the control points.

Thus the average of the abscissae were determined with the standard deviations of about 0.3 unit of the scale of the recording paper, or 0.05° of position angle. The scale could be considered to be the same throughout all the frames without any serious error. Since the mean errors are equal to 0.01°, it is expected that the comparison with Watts' contour are made with a very good agreement.

8) Reading of the photographic densities

The next step in the flowchart for the reduction is to read the ordinates or the photographic densities D from the photometric profiles. Now we have a common origin and the same scale for all the frames. So, if we read the densities for corres-

ponding abscissae x of the successive frames, it is likely that we can follow the change in the density for that point with respect to time. The deviations of the abscissae of the control points, however, amount to 0.12° at maximum, while it should be noticed that the slopes on the moon's contour are generally very steep and often exceed 0.5 unit of D per 0.2° in the profiles. Therefore, if the origin of each frame is simply made coincide with each other, the deviations in the measured densities would be so large that the time dependency is rendered very obscure and consequently it would not lead to a good result.

In order to avoid this difficulty it is advisable that the corresponding control points in the successive profiles are superposed on each other and always the values at the same point are read.

Since this means simply to return the images of hills or valleys in any frame which are carried to arbitrary places by various causes, to their respective mean places, the position angles will not be shifted systematically in this process.

Densities D were read only for the values between 0.97 and 1.47, within which the linearity was kept well. The numbers of the points on which the densities D were read were 124 for the second contact and 138 for the third contact.

9) Determination of t_c

In the process of measuring the densities D , about 15 readings were obtained for every contour point. Since their decrease (for the second contact) and increase (for the third contact) are almost proportional to time, a simple relation is assumed between the density change and time, that is,

$$D = at + b,$$

and from this expression is determined the time t_c at which D takes a certain value. Adopted value of D was 1.22 actually.

Now a slight correction is necessary to the raw data of the density D read from the profile. The density which is needed must be the value as integrated along the radius for each position angle of the crescent. On the other hand, the measured density D is the value summed up on the flash spectrum along the direction of dispersion

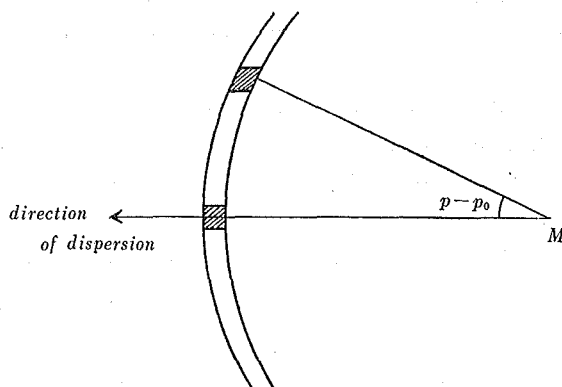


Fig. 6 The intensity is integrated along the direction of the dispersion.

or the value integrated with some inclination to the radius when the position angle is different from the direction of dispersion (Fig. 6).

Let I be the intensity of the spectrum at the position angle p , I_0 being the value integrated in parallel with the direction of dispersion p_0 . I_0 denotes the reduced intensity integrated along the radius. Then obviously from the figure,

$$I_0 = I \cos(p - p_0).$$

On the other hand, D and $\log I$ are connected by a relation, which is approximately expressed as $dD/d \log I = 0.7$. Therefore, the scheme for obtaining reduced density from D is shown in the following way.

$$D \rightarrow \log I \rightarrow I \rightarrow I_0 \rightarrow \log I_0 \rightarrow \text{reduced } D$$

The direction of dispersion p_0 can be determined from the coronal stripes which appear on the both sides in the photographs of the spectrum.

Each t_0 was determined with the mean error of 0.015°. The coefficients a which represent the rate of the density change with time showed unexpected deviations. This is supposed to be caused by the fact that the images on the film suffer the influence of the neighboring light because of the small size of the images. But the results of a preliminary reduction did not show any considerable correlation between the values of a and the amounts of residual. Hence, in the present investigation any correction was not given as to a and all the contour points were treated with an equal weight. The times t_0 for all the adopted points are shown in Table 4.

10) Reading of Watts' charts

From the Astronomical Ephemeris 1970 we obtain the following ephemeris for physical observation for Puerto Escondido at the time of totality,

$$\begin{aligned} l &= +2.70^\circ, \\ b &= -0.15^\circ, \\ C &= 338.63^\circ. \end{aligned}$$

With the use of these values, the heights of the moon's contours above the mean level were read from the charts for every 0.2° in the position angle. Since the values h_M thus read are those at the mean distance of the moon, they must be multiplied by the factor S/S_0 , where S is the moon's topocentric semidiameter, 1006.8" in the present case, and S_0 is 932.6", the semidiameter at the mean distance.

11) Comparison between the observed profiles and Watts' contours—Determination of the position angles

The density is read with respect to the argument x which is the abscissae on the recording paper of the microphotometer. On the other hand, we must know the density with respect to the position angles. The relation between x and the position angles is obtained by comparing the observed profiles with Watts' contours.

With x_0 is denoted the value of x corresponding to the direction of dispersion (or that near to it) and with p_0 and $\left(\frac{dp}{dx}\right)_0$ the position angle and its derivative at x_0 respectively. Let $x^{(i)}$ be x for the i -th control point determined in Section 7 and $p_w^{(i)}$ the position angle belonging to it read from Watts' charts. Then,

$$x^{(i)} - x_0 = r \sin(p_w^{(i)} - p_0),$$

$$r = 57.29578^\circ / \left(\frac{dp}{dx} \right)_0,$$

where p is expressed in degrees.

From 18 control points for each contact, p_0 and $\left(\frac{dp}{dx} \right)_0$ were determined as following.

TABLE 2. CONSTANTS FOR THE CONVERSION x TO p

Contact	x_0	p_0 (m.e.)	$\left(\frac{dp}{dx} \right)_0$ (m.e.)
second	104.57	$28.95^\circ \pm 0.03^\circ$	$0.1573^\circ \pm 0.0012^\circ$
third	126.67	244.12 ± 0.05	-0.1569 ± 0.0011

In Table 4 $p_w^{(1)}$ and $p^{(1)}$ are shown, the latter being calculated from each $x^{(1)}$ using p_0 and $\left(\frac{dp}{dx} \right)_0$ determined above. We can see from Table 4 the deviations as large as 0.3° at the maximum between the observed position angles $p^{(1)}$ and those by Watts $p_w^{(1)}$.

TABLE 3. POSITION ANGLES OF THE "CONTROL POINTS"

$$(\pi = p - C = p + 21.370^\circ)$$

second contact		third contact	
$\pi^{(1)}$	$\pi_w^{(1)}$	$\pi^{(1)}$	$\pi_w^{(1)}$
35.812°	35.810°	256.571°	256.366°
42.432	42.757	257.111	256.822
43.856	43.888	257.533	257.779
44.528	44.403	264.586	264.640
45.147	45.161	265.013	265.125
45.413	45.493	266.633	266.549
46.043	46.041	268.142	267.890
48.586	48.581	268.942	268.769
48.977	49.995	270.781	270.625
49.423	49.479	271.550	271.271
50.900	50.840	271.885	272.949
51.560	51.373	272.183	272.298
51.761	51.577	272.636	272.794
52.900	52.837	273.195	273.205
53.492	53.672	274.380	274.401
54.409	54.301	276.060	275.981
58.070	58.243	276.607	276.459
58.917	58.938	277.900	277.896

12) Revisions to Watt's charts

In comparing the obtained contours with Watts' charts, it is expected that it will give a much better result to compare the both after making some revisions to Watts' values than to do so with the original values. Of course it must be avoided that the position angles are displaced systematically or the zero level is shifted by these revisions.

sions. Two revisions are effective :

i) To give flexibility to the position angles of Watts' charts

As stated in the previous subsection, there exist fairly large deviations in the position angles of the hills and valleys between those observed and those by Watts. Considering the steepness of the lunar topography, it would only produce larger residuals to compare them directly, and it would lead to a rather wrong result. Therefore a small revision is given to the position angle of each control point in Watts' charts so that it coincides with that obtained from observation. Between the control points the scales of position angles are enlarged or contracted in such a way that a linear scale is gained in each interval.

Perhaps it would be more reasonable to give corrections to the observed position angles if we consider that the differences are caused by the image distortions on our film. But the result will be quite the same whichever procedure is taken, since both the position angles are kept coincident with each other on the average. Moreover, for the convenience of any recalculation with the another contour map, it is desirable to remain the observational data unchanged.

ii) Correction to the effects of irradiation

It is obvious that the observed profiles suffer the influences of irradiation etc. because of the resolution power of the optics, the atmospheric disturbance, the emulsion properties and the finiteness of the slit of the microphotometer.

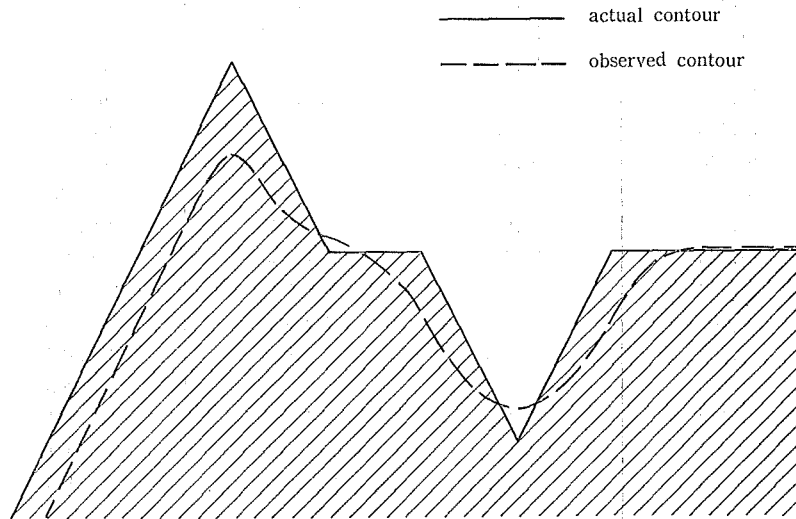


Fig. 7 Simulation of the irradiation effects

In Fig. 7 is shown an example of those effects which is artificially made by a simple simulation by the computer. (The effects are a little exaggerated in this example.) Based on this result is introduced an expression for the correction which is very simple but represents the actual phenomenon with a good agreement, and with

this correction the second revision is made to Watts' contours.

TABLE 4. OBSERVATION DATA

1st column: position angles (not corrected),
 2nd column: t_c in the serial seconds counted from 17^h27^m00^s UTC,
 3rd column: observed heights h ,
 4th column: Watts' heights h_w which are given two revisions already,
 5th column: residuals h' .
 The blanks mean that t_c are not available there.

p	t_c	h	h_w	h'	p	t_c	h	h_w	h'
14.06°	12.58 ^s	-0.87''	-0.83''	-0.04''	23.98°	13.69 ^s	-0.23°	-0.17''	-0.06''
14.22	12.93	-0.96	-0.89	-0.07	24.13	13.75	-0.25	-0.17	-0.08
14.39	13.03	-0.96	-0.92	-0.04	24.29	13.62	-0.19	-0.15	-0.04
14.55	12.98	-0.93	-0.96	+0.03	24.45	13.35	-0.09	-0.11	+0.02
14.71	12.96	-0.89	-0.92	+0.03	24.61	13.11	+0.01	-0.11	+0.12
14.87	12.94	-0.85	-0.85	+0.00	24.77	13.09	+0.02	-0.05	+0.07
19.85			+0.17		24.92	13.32	-0.06	-0.07	+0.01
20.01			+0.03		25.08	13.52	-0.13	-0.18	+0.05
20.17	12.98	-0.22	-0.13	-0.09	25.24	13.87	-0.25	-0.28	+0.03
20.33	13.22	-0.28	-0.21	-0.07	25.40	14.23	-0.37	-0.35	-0.02
20.49	13.55	-0.39	-0.28	-0.11	25.55	14.46	-0.47	-0.44	-0.03
20.65	13.94	-0.52	-0.40	-0.12	25.71	14.72	-0.55	-0.48	-0.07
20.81	14.33	-0.64	-0.55	-0.09	25.87	14.93	-0.62	-0.56	-0.06
20.97	14.91	-0.84	-0.75	-0.09	26.03	14.94	-0.63	-0.74	+0.11
21.13	15.33	-0.98	-0.86	-0.12	26.18	15.08	-0.68	-0.81	+0.13
21.29	15.62	-1.07	-0.91	-0.16	26.34	15.40	-0.80	-0.93	+0.13
21.44	15.55	-1.02	-0.99	-0.03	26.50	15.79	-0.94	-1.03	+0.09
21.60	15.54	-1.01	-1.03	+0.02	26.66	15.92	-0.98	-1.07	+0.09
21.76	15.56	-1.01	-1.03	+0.02	26.81	15.88	-0.97	-1.13	+0.16
21.92	15.40	-0.95	-1.02	+0.07	26.97	15.89	-0.98	-1.17	+0.19
22.08	15.06	-0.81	-0.96	+0.15	27.13	16.04	-1.03	-1.17	+0.14
22.24	14.77	-0.70	-0.85	+0.15	27.29	15.93	-0.99	-1.20	+0.21
22.40	14.50	-0.59	-0.71	+0.12	27.44	15.92	-0.99	-1.25	+0.26
22.55	14.49	-0.58	-0.57	-0.01	27.60	16.38	-1.16	-1.19	+0.03
22.71	14.71	-0.65	-0.57	-0.08	27.76	16.26	-1.11	-1.16	+0.05
22.87	15.14	-0.80	-0.65	-0.15	27.92	15.79	-0.95	-1.13	+0.18
23.03	15.20	-0.81	-0.63	-0.18	28.07	15.54	-0.86	-1.09	+0.23
23.19	15.03	-0.74	-0.62	-0.12	28.23	15.79	-0.95	-1.10	+0.15
23.34	14.78	-0.65	-0.53	-0.12	28.39	16.15	-1.09	-1.15	+0.06
23.50	14.33	-0.48	-0.38	-0.10	28.55	16.27	-1.14	-1.24	+0.10
23.66	13.82	-0.29	-0.25	-0.04	28.70	16.43	-1.20	-1.29	+0.09
23.82	13.63	-0.21	-0.20	-0.01	28.86	16.49	-1.23	-1.29	+0.06

p	t_c	h	h_w	h'
29.02°	16.44 ^s	-1.21''	-1.28''	+0.07''
29.17	16.23	-1.15	-1.21	+0.06
29.33	15.88	-1.01	-1.15	+0.14
29.49	15.59	-0.91	-1.11	+0.20
29.65	15.95	-1.05	-1.09	+0.04
29.80	16.12	-1.12	-1.09	-0.03
29.96	15.95	-1.06	-1.14	+0.08
30.12	16.08	-1.12	-1.15	+0.03
30.28	16.39	-1.24	-1.11	-0.13
30.43	16.20	-1.18	-1.08	-0.10
30.59	16.04	-1.12	-1.00	-0.12
30.75	15.88	-1.07	-0.89	-0.18
30.91	15.51	-0.94	-0.79	-0.15
31.06	15.24	-0.85	-0.73	-0.12
31.22	15.09	-0.80	-0.71	-0.09
31.38	14.96	-0.76	-0.69	-0.07
31.54	15.06	-0.81	-0.69	-0.12
31.69	15.19	-0.87	-0.73	-0.14
31.85	15.26	-0.90	-0.83	-0.07
32.01	15.32	-0.94	-0.93	-0.01
32.17	15.44	-0.99	-0.97	-0.02
32.32	15.62	-1.07	-0.99	-0.08
32.48	15.51	-1.04	-1.00	-0.04
32.64	15.26	-0.96	-0.99	+0.03
32.80	15.04	-0.89	-0.97	+0.08
32.95	15.02	-0.89	-0.94	+0.05
33.11	15.09	-0.93	-0.93	+0.00
33.27	14.96	-0.89	-0.92	+0.03
33.43	14.89	-0.88	-0.92	+0.04
33.59	14.86	-0.87	-0.88	+0.01

p	t_c	h	h_w	h'
33.74°	14.64 ^s	-0.81''	-0.86''	+0.05''
33.90	14.51	-0.78	-0.83	+0.05
34.06	14.48	-0.78	-0.77	-0.01
34.22	14.43	-0.77	-0.73	-0.04
34.37	14.35	-0.76	-0.76	+0.00
34.53	14.27	-0.74	-0.72	-0.02
34.69	14.17	-0.72	-0.66	-0.06
34.85	13.99	-0.66	-0.64	-0.02
35.01	13.75	-0.59	-0.59	+0.00
35.17	13.55	-0.53	-0.49	-0.04
35.32	13.31	-0.45	-0.42	-0.03
35.48	13.08	-0.38	-0.39	+0.01
35.64	12.98	-0.36	-0.37	+0.01
35.80	12.89	-0.35	-0.36	+0.01
35.96	12.81	-0.33	-0.37	+0.04
36.12	13.09	-0.46	-0.39	-0.07
36.27	13.14	-0.50	-0.40	-0.10
36.43	13.16	-0.53	-0.39	-0.14
36.59	13.13	-0.53	-0.33	-0.20
36.75			-0.36	
36.91			-0.42	
37.07	12.46	-0.33	-0.52	+0.19
37.23	13.24	-0.65	-0.71	+0.06
37.39	13.57	-0.80	-0.85	+0.05
37.55	13.62	-0.84	-0.89	+0.05
37.70	13.57	-0.84	-0.89	+0.05
37.86	13.50	-0.84	-0.84	+0.00
38.02	13.41	-0.82	-0.65	-0.17
38.18	13.21	-0.77	-0.55	-0.22
38.34			-0.42	

p	t_c	h	h_w	h'
234.30°	215.18 ^s	+0.33''	+0.19''	+0.14''
234.45	214.62	+0.13	+0.03	+0.10
234.61	214.13	-0.04	-0.13	+0.09
234.77	213.97	-0.08	-0.30	+0.22
234.93	213.83	-0.11	-0.32	+0.21
235.09	213.86	-0.10	-0.31	+0.21
235.25	213.98	-0.04	-0.30	+0.26

p	t_c	h	h_w	h'
235.41°	213.98 ^s	-0.02''	-0.08''	+0.06''
235.57	213.86	-0.06	-0.05	-0.01
235.72	213.69	-0.11	-0.10	-0.01
235.88	213.46	-0.18	-0.15	-0.03
236.04	213.21	-0.27	-0.21	-0.06
236.20	213.22	-0.25	-0.24	-0.01
236.36	213.20	-0.25	-0.25	+0.00

p	t_c	h	h_w	h'	p	t_c	h	h_w	h'
236.52°	213.02 ^s	-0.31''	-0.23''	-0.08''	245.64°	213.52 ^s	-0.02''	+0.04''	-0.06''
236.68	213.21		-0.19	-0.03	245.79	213.47	-0.05	-0.03	-0.02
236.83	213.41	-0.22	-0.16	+0.02	245.95	213.24	-0.14	-0.06	-0.08
236.99	213.94	-0.14	-0.01	+0.09	246.11	213.16	-0.17	-0.16	-0.01
237.15		+0.08	+0.07		246.26	212.53	-0.41	-0.35	-0.06
237.31			+0.13		246.42	211.90	-0.65	-0.55	-0.10
237.47			+0.25		246.58	211.75	-0.71	-0.65	-0.06
240.62			+1.02		246.74	211.74	-0.72	-0.64	-0.08
240.77			+0.81		246.89	211.90	-0.67	-0.59	-0.08
240.93	214.51	+0.43	+0.68	-0.25	247.05	212.74	-0.38	-0.43	+0.05
241.09	214.33	+0.37	+0.61	-0.24	247.21	213.57	-0.10	-0.05	-0.05
241.24	214.39	+0.39	+0.49	-0.10	247.36	214.15	+0.10	+0.12	-0.02
241.40	214.05	+0.26	+0.34	-0.08	247.52	214.18	+0.10	+0.19	-0.09
241.56	213.51	+0.07	+0.19	-0.12	247.68	213.36	-0.20	+0.10	-0.30
241.71	213.15	-0.06	+0.05	-0.11	247.84	212.93	-0.37	-0.19	-0.18
241.87	212.67	-0.24	-0.08	-0.16	247.99	212.78	-0.43	-0.33	-0.10
242.03	212.21	-0.42	-0.20	-0.22	248.15	212.59	-0.51	-0.42	-0.09
242.19	211.88	-0.54	-0.33	-0.21	248.31	212.46	-0.57	-0.51	-0.06
242.34	211.63	-0.63	-0.40	-0.23	248.46	212.46	-0.58	-0.61	+0.03
242.50	211.35	-0.73	-0.51	-0.22	248.62	212.25	-0.67	-0.74	+0.07
242.66	210.81	-0.93	-0.74	-0.19	248.78	211.86	-0.82	-0.96	+0.14
242.81	210.36	-1.10	-1.03	-0.07	248.94	211.40	-0.99	-1.17	+0.18
242.97	209.88	-1.27	-1.18	-0.09	249.09	211.07	-1.12	-1.27	+0.15
243.13	209.59	-1.38	-1.28	-0.10	249.25	210.98	-1.17	-1.28	+0.11
243.28	209.54	-1.40	-1.32	-0.08	249.41	210.98	-1.19	-1.29	+0.10
243.44	210.00	-1.23	-1.29	+0.06	249.57	211.46	-1.03	-1.10	+0.07
243.60	210.44	-1.07	-1.23	+0.16	249.72	212.06	-0.83	-0.93	+0.10
243.75	210.60	-1.02	-1.19	+0.17	249.88	212.14	-0.83	-0.87	+0.04
243.91	210.62	-1.01	-1.12	+0.11	250.04	212.08	-0.86	-0.84	-0.02
244.07	210.78	-0.96	-1.08	+0.12	250.20	212.03	-0.89	-0.91	+0.02
244.23	211.10	-0.85	-1.06	+0.21	250.35	212.01	-0.92	-0.96	+0.00
244.38	211.68	-0.64	-0.75	+0.11	250.51	211.87	-0.98	-0.98	+0.04
244.54	212.68	-0.28	-0.53	+0.25	250.67	211.69	-1.06	-0.98	-0.08
244.70	213.55	+0.03	-0.24	+0.27	250.83	211.93	-1.00	-0.99	-0.01
244.85	214.06	+0.21	+0.19	+0.02	250.99	211.91	-1.02	-1.04	+0.02
245.01	214.54	+0.38	+0.39	-0.01	251.14	211.64	-1.13	-1.09	-0.04
245.17	214.95	+0.52	+0.49	+0.03	251.30	211.32	-1.26	-1.13	-0.13
245.32	214.62	+0.39	+0.41	-0.02	251.46	211.26	-1.30	-1.12	-0.18
245.48	213.83	+0.10	+0.21	-0.11	251.62	211.61	-1.20	-1.08	-0.12

p	t_c	h	h_w	h'	p	t_c	h	h_w	h'
251.78°	211.84 ^s	-1.14"	-1.18"	+0.04"	255.44°	213.62 ^s	-1.07"	-1.11"	+0.04"
251.94	211.81	-1.16	-1.10	-0.06	255.60	213.78	-1.05	-1.09	+0.04
252.09	211.55	-1.27	-1.01	-0.26	255.76	213.81	-1.07	-1.09	+0.02
252.25	211.29	-1.38	-1.12	-0.26	255.92	213.85	-1.08	-1.04	-0.04
252.41	211.25	-1.42	-1.33	-0.09	256.08	214.05	-1.05	-1.00	-0.05
252.57	211.22	-1.45	-1.49	+0.04	256.24	214.24	-1.01	-1.01	+0.00
252.73	211.24	-1.46	-1.67	+0.21	256.40	214.48	-0.97	-0.91	-0.06
252.89	210.96	-1.58	-1.81	+0.23	256.56	214.70	-0.92	-0.89	-0.03
253.05	210.49	-1.76	-1.79	+0.03	256.72	214.57	-0.99	-0.88	-0.11
253.20	210.89	-1.65	-1.76	+0.11	256.88	214.59	-1.02	-0.87	-0.15
253.36	211.57	-1.44	-1.68	+0.24	257.04	215.07	-0.90	-0.89	-0.01
253.52	212.24	-1.23	-1.46	+0.23	257.36	215.24	-0.91	-0.92	+0.01
253.68	212.29	-1.24	-1.26	+0.02	257.52	214.99	-1.02	-0.97	-0.05
253.84	212.30	-1.26	-1.27	+0.01	257.68	215.03	-1.04	-0.99	-0.05
254.00	212.51	-1.21	-1.22	+0.01	257.85	215.14	-1.04	-1.07	+0.03
254.16	212.81	-1.14	-1.10	-0.04	258.65	215.18	-1.20	-1.23	+0.03
254.32	213.21	-1.03	-1.01	-0.02	258.82	214.86	-1.33	-1.47	+0.14
254.48	213.68	-0.90	-0.99	+0.09	258.98			-1.58	
254.64	213.96	-0.82	-0.99	+0.17	259.14			-1.67	
254.80	213.79	-0.92	-1.04	+0.12	259.30			-1.77	
254.96	213.49	-1.03	-1.09	+0.06	259.47			-1.86	
255.12	213.44	-1.08	-1.17	+0.09	259.63			-1.96	
255.28	213.50	-1.08	-1.19	+0.11	259.79			-1.95	

13) Least squares solution

In solving the equations for the least squares method (2) and (3), a modification is made to these equations, such that a constant error in the position angles in the contour map, if it ever exists, is detected. The new equations are obtained by substituting $p+u$ for p and introducing another unknown u . After this substitution p means the tabular position angle in Watts' charts and $p+u$ represents the true position angle. The modified equations are

$$ax_2 + by_2 + cu + z_2 = -v \cos(\phi - p) \times (t_c - t_{02}) - h_w - v - h' \quad (\text{for the second contact}), \quad (4)$$

$$ax_2 + by_2 + cu + z_2 = -v \cos(\phi - p) \times (t_c - t_{03}) - h_w - v - h' - a\xi - b\eta - \zeta \quad (\text{for the third contact}),$$

where $c = d_i \sin(p_{0i} - p) + v \sin(\phi - p) \times (t_c - t_{0i}) \quad (i=2, 3).$

The heights h_w are the readings from the Watts' charts and the approximate values for d_i and p_{0i} are taken from the predictions. The other notations are the same as in (2) and (3).

Similarly as to (x', y') ,

$$\begin{aligned}
 a'x'_2 + b'y'_2 + cu + z_2 &= -v \cos(\phi - p) \times (t_c - t_{02}) - h_w - \nu - h' \\
 &\text{(for the second contact),} \\
 a'x'_2 + b'y'_2 + cu + z_2 &= -v \cos(\phi - p) \times (t_c - t_{03}) - h_w - \nu - h' - a\xi - b\eta - \zeta \\
 &\text{(for the third contact).}
 \end{aligned} \tag{5}$$

Table 4 gives the necessary quantities for the solution. Also Fig. 8 shows h and h_w . As for Watts' heights h_w , both the original and the revised ones are given.

Finally the least squares equations are solved, which give the results: at the time $17^{\text{h}} 27^{\text{m}} 15.566^{\text{s}}$ UTC (which is t_{02});

i) in Right Ascension and Declination,

$$\begin{aligned}
 x_2 = \delta_\zeta - \delta_\odot &= -35.36'' \pm 0.05'' \text{ (m.e.)}, \\
 &\text{(-35.51)} \\
 y_2 = (\alpha_\zeta - \alpha_\odot) \cos \delta_\odot &= -17.94 \pm 0.05 \text{ (,,)}, \\
 &\text{(-18.30)} \\
 z_2 = r_\zeta - r_\odot &= +40.50 \pm 0.02 \text{ (,,)}, \\
 &\text{(+40.82)} \\
 u &= +0.17^\circ \pm 0.09^\circ \text{ (,,)}.
 \end{aligned}$$

(The figures in the parentheses are the values calculated from the ephemeris.)

ii) in the directions of the relative motion and rectangular to it ($\phi = 44.77^\circ$),

$$\begin{aligned}
 x'_2 &= -37.733'' \pm 0.008'' \text{ (m.e.)} \\
 &\text{(positive sign is for the direction of } \phi \text{),} \\
 y'_2 &= -12.16 \pm 0.07 \text{ (,,)} \\
 &\text{(positive sign is for the direction } 90^\circ \text{ from } \phi \text{ clockwise),} \\
 z_2 &= +40.50 \pm 0.02 \text{ (,,)} \\
 u &= + 0.17^\circ \pm 0.09^\circ \text{ (,,)}.
 \end{aligned}$$

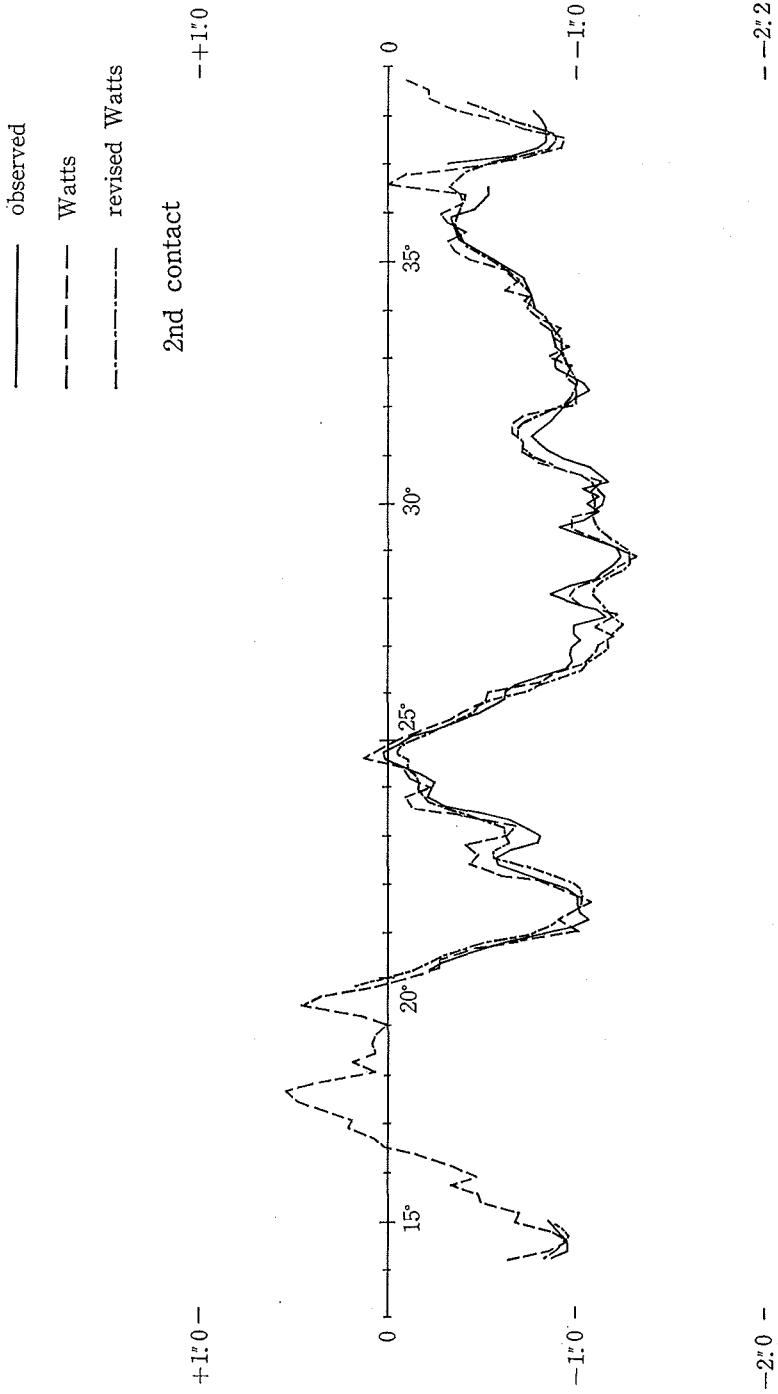
6. Conclusion

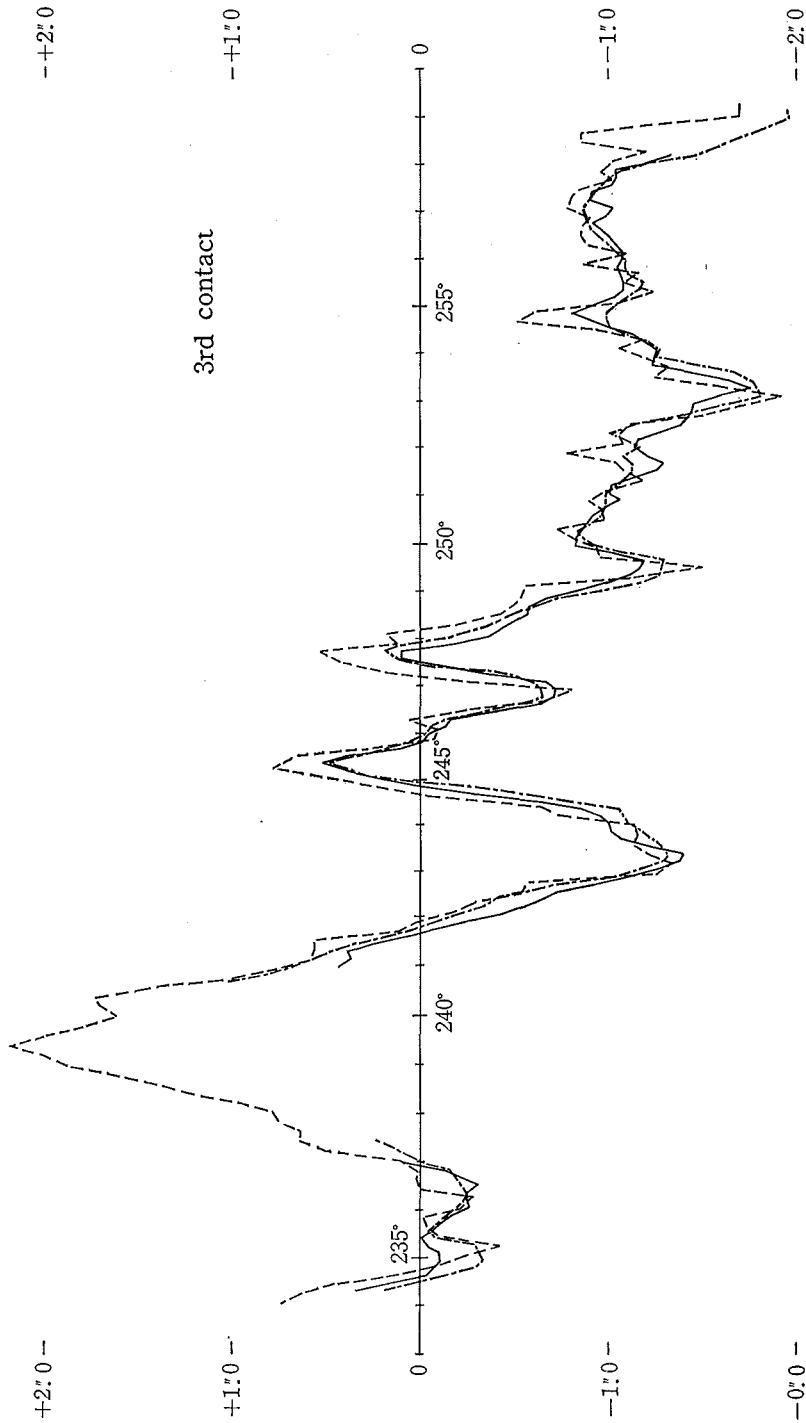
The position of the sun with respect to the moon was derived numerically to the accuracy of $0.008''$ in the direction of the apparent relative motion. Though this accuracy should be reduced to $0.02'' \sim 0.03''$ in view of the fact that it has been yielded by the treatments of somewhat dependent values of lunar contours it is reasonable to say that our initial aim is completely attained when it is reminded that it is the determination of contact with an accuracy comparable to that of the datum provided by the lunar map. However the discrepancies between the two contours, that of Watts and that just derived, are unexpectedly large. They are considered to be brought about by the photographic effects (e.g. irradiation, Eberhard effect) inevitable in such a small system of registration.

The correction to the orientation of Watts' charts is not so reliable because the results are apt to be affected even by small errors in the data. The observation of the eclipse is probably not favorable for this problem

The differences between the observation and the ephemeris, although we can not refer to them definitely due to the lack of knowledge on the exact values of the ephemeris time and the geodetic position of the observation point, do not seem to be

Fig. 8. Contours at second and third contacts





explainable by the observational errors, the vertical deflection at the point and the unestablished part of the ephemeris time.

The authors wish to thank Prof. K. Saito of the Tokyo Astronomical Observatory, Dr. M. Kanno of the Kwasan Observatory and the members of the expedition for helping the observation in Mexico. They also thank to the staff of the Tokyo Astronomical Observatory for arranging the usage of the microphotometer.

References

- Kristenson, H., 1952, *Stockholms Observatoriums Annaler*, Bd. 17, Nr. 1.
Kristenson, H., 1959, *ARKIV FOR ASTRONOMI*, Bd. 2, Nr. 29.
Watts, C. B., 1963, *Astr. Pap. Amer. Eph.*, 17.